EDISON

Electromagnetic Design of
flexIble SensOrs

FNP Team-Tech

Report 4. Homogeneous and coaxially loaded cylindrical resonators made from lossy material

BSc. Malgorzata Warecka
August 25, 2017

European Funds Smart Growth

FNP Foundation for Polish Science

European Union
European Regional Development Fund

This work was supported by project EDISOn - Electromagnetic Design of flexIbleSensOrs, *The „EDISOn" project is carried out within the TEAM-TECH programme programme of the Foundation for Polish Science co-financed by the European Union under the European Regional Development Fund.*

Revision	Date	Author(s)	Description
1.0	25.08.2017	M. Warecka	created

1 Introduction

The aim of the report is to show the results of analysis for two closed structures: homogeneous and coaxially loaded cylindrical resonators presented in the Fig. 1.

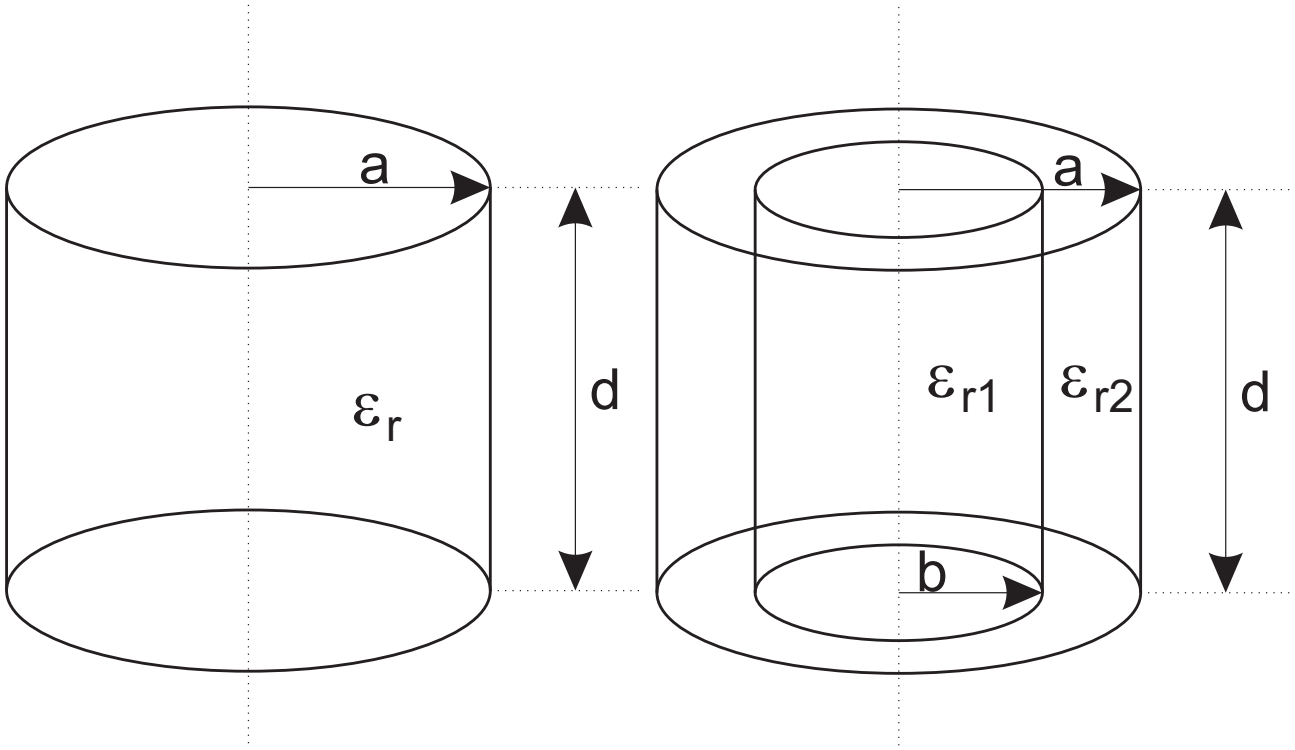

Figure 1: Homogeneous (left) and coaxially loaded (right) cylindrical resonators.

The first considered cylindrical resonator is fully filled with lossy material. The second (coaxially loaded) resonator can be divided into two regions. The first area is a lossy layer and the second one is a vacuum. The permittivity of lossy material can be expressed as $\varepsilon_r = 10 - j\epsilon''$. Results of the analysis are presented in the next sections. For all calculations constants have value $c = 2.99792458 \cdot 10^8 \frac{m}{s}$ and $\mu_0 = 4\pi 10^{-7} \frac{H}{m}$, the tolerance of finding zeros by using root finding algorithm is 10^{-10}.

2 Problem formulation

Maxwell's equations determine character of fields. The fields for cylindrical resonators have the following form:

$$\widehat{E_z} = E_z(\rho)cos(m\phi)cos(\frac{l\pi}{d}z) \tag{1}$$

$$\widehat{E_\rho} = E_\rho(\rho)cos(m\phi)sin(\frac{l\pi}{d}z) \tag{2}$$

$$\widehat{E_\phi} = E_\phi(\rho)sin(m\phi)sin(\frac{l\pi}{d}z) \tag{3}$$

$$\widehat{H_z} = H_z(\rho)sin(m\phi)sin(\frac{l\pi}{d}z) \tag{4}$$

$$\widehat{H_\rho} = H_\rho(\rho)sin(m\phi)cos(\frac{l\pi}{d}z) \tag{5}$$

$$\widehat{H_\phi} = H_\phi(\rho)cos(m\phi)cos(\frac{l\pi}{d}z) \tag{6}$$

where m, n and l refer to the field variation with respect to ϕ, ρ and z, respectively. The boundary conditions can be written as:

$$\frac{\partial \widehat{E_z}(\rho,\phi,d)}{\partial z} = 0 \tag{7}$$

$$\frac{\partial \widehat{E_z}(\rho,\phi,0)}{\partial z} = 0 \tag{8}$$

$$E_\phi(\rho,\phi,d) = 0 \tag{9}$$

$$E_\phi(\rho,\phi,0) = 0 \tag{10}$$

$$E_\phi(a,\phi,z) = 0 \tag{11}$$

$$E_z(a,\phi,z) = 0 \tag{12}$$

2.1 Homogeneous cylindrical resonators

The equations for the homogeneous resonator can be separated. Direct consequences of the separation of equations are transverse magnetic and electric modes in the resonator.

For TM_{mnl} modes, fields can be expressed as:

$$E_\rho(\rho) = -\frac{jl\pi}{d\kappa}AJ'_m(\kappa\rho) \tag{13}$$

$$E_\phi(\rho) = \frac{l\pi m}{d\kappa^2\rho}AJ_m(\kappa\rho) \tag{14}$$

$$E_z(\rho) = AJ_m(\kappa\rho) \tag{15}$$

$$H_\rho(\rho) = -\frac{j\omega\varepsilon m}{\kappa^2\rho}AJ_m(\kappa\rho) \tag{16}$$

$$H_\phi(\rho) = -\frac{\omega\varepsilon m}{\kappa}AJ_m(\kappa\rho) \tag{17}$$

$$H_z(\rho) = 0 \tag{18}$$

and for TE_{mnl} modes :

$$E_\rho(\rho) = \frac{\omega\mu m}{\rho\kappa^2}AJ_m(\kappa\rho) \tag{19}$$

$$E_\phi(\rho) = \frac{\omega\mu}{\kappa}AJ'_m(\kappa\rho) \tag{20}$$

$$E_z(\rho) = 0 \tag{21}$$

$$H_\rho(\rho) = -\frac{jl\pi}{d\kappa}AJ'_m(\kappa\rho) \tag{22}$$

$$H_\phi(\rho) = \frac{jl\pi m}{d\kappa^2\rho}AJ_m(\kappa\rho) \tag{23}$$

$$H_z(\rho) = -jAJ_m(\kappa\rho) \tag{24}$$

where $\kappa^2 = (\frac{2\pi f}{c})^2\varepsilon_r + (\frac{jl\pi}{d})^2$, J_m is the Bessel function, Y_m is the Neumann function. Use of the boundary conditions is reduced to finding zeros of the presented equation:

- TM modes

$$J_m(\kappa a) = 0 \tag{25}$$

- TE modes

$$J'_m(\kappa a) = 0 \tag{26}$$

2.2 Coaxially loaded cylindrical resonator

If we consider the coaxially loaded cylindrical resonator, then the fields can be expressed as:

$$E_z^I(\rho) = A^I J_m(\kappa_1 \rho) \tag{27}$$

$$E_\phi^I(\rho) = \frac{l\pi m}{d\kappa_1^2 \rho} A^I J_m(\kappa_1 \rho) + \frac{j\omega\mu_1}{\kappa_1} C^I J'_m(\kappa_1 \rho) \tag{28}$$

$$H_z^I(\rho) = C^I J_m(\kappa_1 \rho) \tag{29}$$

$$H_\phi^I(\rho) = \frac{l\pi m}{d\kappa_1^2 \rho} C^I J_m(\kappa_1 \rho) - \frac{j\omega\varepsilon_1}{\kappa_1} A^I J'_m(\kappa_1 \rho) \tag{30}$$

for the first region and

$$E_z^{II}(\rho) = A^{II} J_m(\kappa_2 \rho) + B^{II} Y_m(\kappa_2 \rho) \tag{31}$$

$$E_\phi^{II}(\rho) = \frac{l\pi m}{d\kappa_2^2 \rho} A^{II} J_m(\kappa_2 \rho) + \frac{l\pi m}{d\kappa_2^2 \rho} B^{II} Y_m(\kappa_2 \rho) + \frac{j\omega\mu_2}{\kappa_2} C^{II} J'_m(\kappa_2 \rho) + \frac{j\omega\mu_2}{\kappa_2} D^{II} Y'_m(\kappa_2 \rho) \tag{32}$$

$$H_z^{II}(\rho) = C^{II} J_m(\kappa_2 \rho) + D^{II} Y_m(\kappa_2 \rho) \tag{33}$$

$$H_\phi^{II}(\rho) = \frac{l\pi m}{d\kappa_2^2 \rho} C^{II} J_m(\kappa_2 \rho) + \frac{l\pi m}{d\kappa_2^2 \rho} D^{II} Y_m(\kappa_2 \rho) + \frac{j\omega\mu_2}{\kappa_2} A^{II} J'_m(\kappa_2 \rho) + \frac{j\omega\mu_2}{\kappa_2} B^{II} Y'_m(\kappa_2 \rho) \tag{34}$$

for the second region. The resonance frequencies for this structure can be found also from boundary conditions, by finding the roots of the following determinant:

$$\begin{vmatrix} J_m(\kappa_1 a) & 0 & -J_m(\kappa_2 a) & -Y_m(\kappa_2 a) & 0 & 0 \\ 0 & J_m(\kappa_1 a) & 0 & 0 & -J_m(\kappa_2 a) & -Y_m(\kappa_2 a) \\ -\frac{j\omega\varepsilon_1}{\kappa_1} J'_m(\kappa_1 a) & \frac{l\pi m}{da\kappa_1^2} J_m(\kappa_1 a) & \frac{j\omega\varepsilon_2}{\kappa_2} J'_m(\kappa_2 a) & \frac{j\omega\varepsilon_2}{\kappa_2} Y'_m(\kappa_2 a) & -\frac{l\pi m}{da\kappa_2^2} J_m(\kappa_2 a) & -\frac{l\pi m}{da\kappa_2^2} Y_m(\kappa_2 a) \\ \frac{l\pi m}{da\kappa_1^2} J_m(\kappa_1 a) & \frac{j\omega\mu_1}{\kappa_1} J'_m(\kappa_1 a) & -\frac{l\pi m}{da\kappa_2^2} J_m(\kappa_2 a) & -\frac{l\pi m}{da\kappa_2^2} Y_m(\kappa_2 a) & -\frac{j\omega\mu_2}{\kappa_2} J'_m(\kappa_2 a) & -\frac{j\omega\mu_2}{\kappa_2} J'_m(\kappa_2 a) \\ 0 & 0 & \frac{l\pi m}{db\kappa_2^2} J_m(\kappa_2 b) & \frac{l\pi m}{db\kappa_2^2} Y_m(\kappa_2 b) & \frac{j\omega\mu_2}{\kappa_2} J'_m(\kappa_2 b) & \frac{j\omega\mu_2}{\kappa_2} J'_m(\kappa_2 b) \\ 0 & 0 & J_m(\kappa_2 b) & Y_m(\kappa_2 b) & 0 & 0 \end{vmatrix} = 0 \tag{35}$$

3 Results

3.1 Homogeneous cylindrical resonator

This section presents results for transverse magnetic and transverse electric modes in the homogeneous cylindrical resonator. The imaginary part of the permittivity was changed in the range between 0 and 10000. The illustration of the structure is presented in the Fig. 1. The geometrical dimensions used in the global root finding algorithm are $d = 10\sqrt{2}mm$ and $a = 10mm$. The form of the mode can be described as $TM_{(mnl)}$ or $TE_{(mnl)}$, where m, n and l refer to the field variation with respect to ϕ, ρ and z, respectively. The analysed modes are described in the table 2. The complex resonance frequency as a function of losses is presented in the Fig. 2-4. The resonance frequency for $\varepsilon_r = 10$ is shown in the table 3.1. The results from the global root finding algorithm have been placed in the table 3.1. The initial mesh step in the global root finding algoritm was set to 0.01 [1].

3.2 Coaxially loaded cylindrical resonator

This section demonstrates the results for modes in a coaxially loaded cylindrical resonator. The imaginary part of the permittivity was changed in the range between 0 and 10000. The illustration of the structure is presented in the Fig. 1. The geometrical dimensions used in the analysis are $d = 10\sqrt{2}mm$, $a = 6.35mm$ and $b = 10mm$. The form of the mode can be described as in the previous section. The analysed modes are described in the table 5. The complex resonance frequency as a function of losses is presented in the Fig. 5-7. The resonance frequency for $\varepsilon_{r2} = 1$ and $\varepsilon_{r1} = 10$ is shown in the table 3.1. The results of the analysis is found in the table 3.2. The initial mesh step in the global root finding algoritm was set to 0.01 [1].

Table 2: Modes presented in Fig.2-4.

mode	color in figure	line style
TE_{011}	red	solid
TE_{012}	green	solid
TE_{111}	black	solid
TE_{112}	cyan	solid
TE_{121}	magenta	solid
TE_{211}	yellow	solid
TE_{212}	blue	dotted
TE_{311}	red	dotted
TE_{411}	green	dotted
TM_{010}	black	dotted
TM_{011}	cyan	dotted
TM_{012}	magenta	dotted
TM_{020}	yellow	dotted
TM_{021}	blue	dashed
TM_{110}	red	dashed
TM_{111}	green	dashed
TM_{112}	black	dashed
TM_{210}	cyan	dashed
TM_{211}	magenta	dashed
TM_{310}	yellow	dashed

	$\varepsilon_{r2} = 10$	$\varepsilon_{r2} = 1$	
TM_{010}	3.628477324	3.883856934	TM_{010}
TE_{111}	4.353381158	6.088975322	HE_{111}
TM_{011}	4.939664708	8.193372828	TM_{011}
TE_{211}	5.698345714	9.884743615	HE_{211}
TM_{110}	5.781399895	6.618765916	TM_{110}
TM_{111}	6.682740791	9.884743615	EH_{111}
TE_{011}	6.682740791	7.575026719	HE_{011}
TE_{311}	7.170490584	12.308462125	HE_{311}
TE_{112}	7.256393506	8.439295609	HE_{112}
TM_{012}	7.622572179	10.941790074	TM_{012}
TM_{210}	7.748790347	9.389886432	TM_{210}
TE_{212}	8.134768778	10.796266012	HE_{212}
TM_{020}	8.328869505	10.120293653	TM_{020}
TM_{211}	8.442641268	12.403656676	EH_{211}
TE_{411}	8.695267456	15.220919382	HE_{411}
TE_{121}	8.714608766	11.393804922	HE_{121}
TE_{012}	8.852250769	9.8095604466	HE_{012}
TM_{112}	8.852250769	12.101986836	EH_{112}
TM_{021}	8.978001279	12.187616669	TM_{021}
TM_{310}	9.626591289	12.204096657	TM_{310}

Table 3: A resonance frequency of the homogeneous resonator as a function of the loss coefficient.

ϵ''	1	5
TM_{010}	3.614968939 + 0.180298821i	3.339803162 + 0.788420577i
TE_{111}	4.337174043 + 0.216319249i	4.007035144 + 0.945932682i
TM_{011}	4.921274929 + 0.245451643i	4.546675185 + 1.073324415i
TE_{211}	5.677131457 + 0.283150457i	5.244997097 + 1.238175856i
TM_{110}	5.759876437 + 0.287277414i	5.321443659 + 1.256222442i
TM_{111}	6.657861749 + 0.332064990i	6.151075735 + 1.452072008i
TE_{011}	6.657861749 + 0.332064990i	6.151075735 + 1.452072008i
TE_{311}	7.143795708 + 0.356301248i	6.600021162 + 1.558053647i
TE_{112}	7.229378824 + 0.360569759i	6.679089825 + 1.576719226i
TM_{012}	7.594194258 + 0.378765155i	7.016136079 + 1.656285054i
TM_{210}	7.719942531 + 0.385036928i	7.132312590 + 1.683710608i
TE_{212}	8.104484011 + 0.404216173i	7.487583374 + 1.767578663i
TM_{020}	8.297862124 + 0.413861027i	7.666241848 + 1.809754208i
TM_{211}	8.411210328 + 0.419514339i	7.770962165 + 1.834475321i
TE_{411}	8.662896020 + 0.432067319i	8.003489935 + 1.889367682i
TE_{121}	8.682165324 + 0.433028388i	8.021292490 + 1.893570295i
TE_{012}	8.825400373 + 0.440172325i	8.153624712 + 1.924809695i
TM_{112}	8.819294902 + 0.439867811i	8.147983980 + 1.923478098i
TM_{021}	8.944577258 + 0.446116346i	8.263730039 + 1.950802036i
TM_{310}	9.590752646 + 0.478344745i	8.860719567 + 2.091732147i

ϵ''	10	50
TM_{010}	2.818916816 + 1.167633576i	1.242661241 + 1.018738535i
TE_{111}	3.382085171 + 1.400905547i	1.490922376 + 1.222263982i
TM_{011}	3.837561231 + 1.589569908i	1.691709587 + 1.386870122i
TE_{211}	4.426970632 + 1.833711276i	1.951538545 + 1.599878915i
TM_{110}	4.491494345 + 1.860437873i	1.979982491 + 1.623197373i
TM_{111}	5.191734358 + 2.150486783i	2.288668834 + 1.876259642i
TE_{011}	5.191734358 + 2.150486783i	2.288668834 + 1.876259642i
TE_{311}	5.570660825 + 2.307443265i	2.455710739 + 2.013201247i
TE_{112}	5.637397687 + 2.335086578i	2.485130306 + 2.037319523i
TM_{012}	5.921877133 + 2.452921823i	2.610537192 + 2.140128578i
TM_{210}	6.019934386 + 2.493538467i	2.653763706 + 2.175565843i
TE_{212}	6.319796006 + 2.617745217i	2.785951507 + 2.283933918i
TM_{020}	6.470590334 + 2.680206273i	2.852426071 + 2.338430025i
TM_{211}	6.558978137 + 2.716817699i	2.891390008 + 2.370372813i
TE_{411}	6.755240135 + 2.798112081i	2.977908055 + 2.441300645i
TE_{121}	6.770266147 + 2.804336059i	2.984531962 + 2.446730950i
TE_{012}	6.877198428 + 2.848628860i	3.031670849 + 2.485375594i
TM_{112}	6.877198428 + 2.848628860i	3.031670849 + 2.485375594i
TM_{021}	6.974892363 + 2.889095012i	3.074737202 + 2.520681558i
TM_{310}	7.478773501 + 3.097809414i	3.296862792 + 2.702780984i

ϵ''	100	500
TM_{010}	0.848647670 + 0.768015586i	0.366420891 + 0.359165750i
TE_{111}	1.018192053 + 0.921451144i	0.439625127 + 0.430920541i
TM_{011}	1.155315183 + 1.045545871i	0.498830827 + 0.488953967i
TE_{211}	1.332759552 + 1.206130818i	0.575446042 + 0.564052199i
TM_{110}	1.352184708 + 1.223710342i	0.583833248 + 0.572273338i
TM_{111}	1.562995134 + 1.414491156i	0.674854937 + 0.661492796i
TE_{011}	1.562995134 + 1.414491156i	0.674854937 + 0.661492796i
TE_{311}	1.677072663 + 1.517729901i	0.724110230 + 0.709772833i
TE_{112}	1.697164097 + 1.535912399i	0.732785116 + 0.718275956i
TM_{012}	1.782807923 + 1.613418996i	0.769763579 + 0.754522245i
TM_{210}	1.812328503 + 1.640134753i	0.782509690 + 0.767015983i
TE_{212}	1.902603201 + 1.721832233i	0.821487627 + 0.805222156i
TM_{020}	1.948000516 + 1.762916238i	0.841088841 + 0.824435265i
TM_{211}	1.974610064 + 1.786997548i	0.852578055 + 0.835696992i
TE_{411}	2.033695628 + 1.840469248i	0.878089449 + 0.860703260i
TE_{121}	2.038219276 + 1.844563094i	0.880042626 + 0.862617764i
TE_{012}	2.070411724 + 1.873696858i	0.893942370 + 0.876242293i
TM_{112}	2.070411724 + 1.873696858i	0.893942370 + 0.876242293i
TM_{021}	2.099822925 + 1.900313630i	0.906641254 + 0.888689739i
TM_{310}	2.251518623 + 2.037596350i	0.972138957 + 0.952890586i

ϵ''	1000	5000	10000
TM_{010}	0.257845251 + 0.255279691i	0.114857097 + 0.114627613i	0.081175756 + 0.081094621i
TE_{111}	0.309358047 + 0.306279934i	0.137803459 + 0.137528127i	0.097393197 + 0.097295853i
TM_{011}	0.351020269 + 0.347527617i	0.156361884 + 0.156049473i	0.110509446 + 0.110398992i
TE_{211}	0.404933324 + 0.400904237i	0.180377440 + 0.180017046i	0.127482545 + 0.127355126i
TM_{110}	0.410835283 + 0.406747472i	0.183006466 + 0.182640819i	0.129340621 + 0.129211345i
TM_{111}	0.474885972 + 0.470160856i	0.211537828 + 0.211115175i	0.149505286 + 0.149355855i
TE_{011}	0.474885972 + 0.470160856i	0.211537828 + 0.211115175i	0.149505286 + 0.149355855i
TE_{311}	0.509546232 + 0.504476246i	0.226977231 + 0.226523731i	0.160417152 + 0.160256815i
TE_{112}	0.515650627 + 0.510519903i	0.229696433 + 0.229237499i	0.162338959 + 0.162176701i
TM_{012}	0.541671854 + 0.536282219i	0.241287581 + 0.240805489i	0.170531054 + 0.170360608i
TM_{210}	0.550641114 + 0.545162234i	0.245282936 + 0.244792860i	0.173354788 + 0.173181520i
TE_{212}	0.578069343 + 0.572317552i	0.257500833 + 0.256986346i	0.181989840 + 0.181807942i
TM_{020}	0.591862443 + 0.585973410i	0.263644965 + 0.263118203i	0.186332233 + 0.186145994i
TM_{211}	0.599947241 + 0.593977765i	0.267246337 + 0.266712379i	0.188877518 + 0.188688735i
TE_{411}	0.617899252 + 0.611751153i	0.275243055 + 0.274693120i	0.194529234 + 0.194334802i
TE_{121}	0.619273675 + 0.613111902i	0.275855292 + 0.275304133i	0.194961935 + 0.194767070i
TE_{012}	0.629054731 + 0.622795635i	0.280212260 + 0.279652396i	0.198041241 + 0.197843299i
TM_{112}	0.629054731 + 0.622795635i	0.280212260 + 0.279652396i	0.198041241 + 0.197843299i
TM_{021}	0.637990758 + 0.631642749i	0.284192811 + 0.283624994i	0.200854513 + 0.200653759i
TM_{310}	0.684080574 + 0.677273972i	0.304723507 + 0.304114670i	0.215364672 + 0.215149415i